Transport theories applied to the study of convoy-electron production

M. L. Martiarena and C. R. Garibotti
Consejo Nacional de Investigaciones Científicas y Técnicas and Centro Atómico Bariloche, 8400 Bariloche, Argentina
(Received 4 September 1990)

We write a transport equation for the electrons produced when atomic or ionic beams traverse a foil. We consider that the electrons are produced inside the solid by the electron loss and capture-to-continuum mechanisms. They lose energy by inelastic collisions with the target atoms and are deflected by elastic scattering. We study the electron distribution for H^0 and H^+ projectiles on carbon foils for different thicknesses. We obtain a description of the electron-velocity spectra in the forward direction that agrees with the experiments. Studying the ratio between the intrinsic convoy-electron height and the nonconvoy-electron or "background" intensity, at convoy-electron velocity, we obtain a constant behavior for different target thicknesses.

PACS number(s): 34.10.+x, 79.20.−m

I. INTRODUCTION

In the electron spectrum resulting from ion–solid-foil collisions, a sharp peak is observed in the forward direction centered at the same velocity as the incident ion. These electrons that travel away with the ion are called "convoy electrons." The origin of that process is an interesting subject of discussion, and several models have been proposed [1]. Dettmann, Harrison, and Lucas [2] consider a single-collision model where the ion captures one electron into a continuum state (ECC) in the last layer of the foil. This is only qualitatively true, for sufficiently fast protons and thin targets. As a foil never presents a thin target, the electron loss to continuum (ELC) must be considered as a competing process [3]. This ELC process will be effective even for bare incident projectiles.

A completely different model for the production of convoy-foil electrons considers collective properties of the valence-electron plasma in a solid [4]. If the projectile velocity is greater than the Fermi velocity v_F, it is possible that a perturbation of the plasma density stays behind the ion. This perturbation consists of an alternately enhanced and depleted electron density relative to the mean density in the medium, creating regions of negative and positive potential. This wake accompanies the ionic projectile and can trap the electrons into bound states. The production of convoy electrons originating from this "wake-riding" model can be considered as a special case of ELC [3].

The shapes and intensities of convoy-electron spectra as a function of projectile species, energies, and electron ejection angles have been extensively studied experimentally, for foil targets thick enough to attain projectile charge equilibrium [5]. Recently, experiments have been made to study the convoy-electron production when the charge state of the emergent beam is out of equilibrium [6–11]. The typical convoy cusp is observed when bare ions interact with thin target foils, and it almost does not change with increasing foil thickness. When the projectile bears bound electrons an additional hump appears for intermediate foil thicknesses, which broadens and is shifted to low velocities for increasing thickness, as shown in Fig. 1.

Some models have been proposed to describe the two observed features. Yamazaki and Oda [12] consider that the electrons lose their correlation to the moving beam in

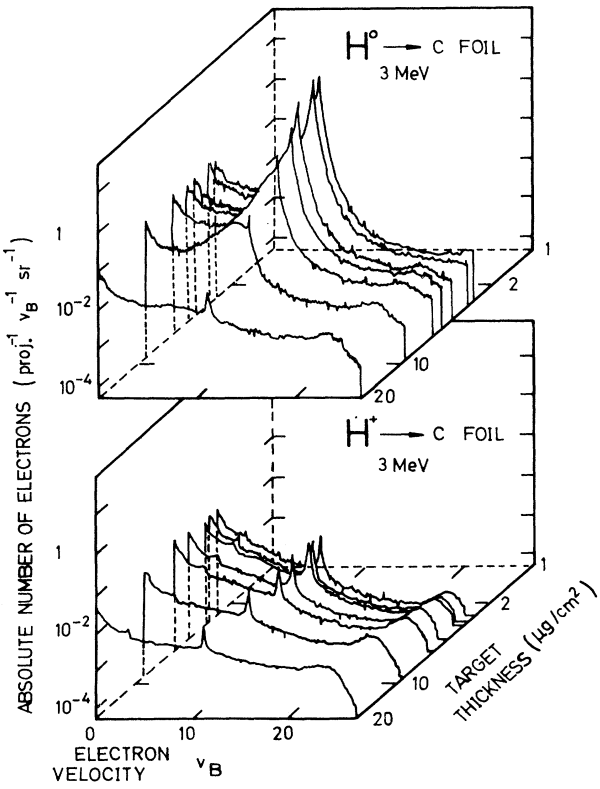

FIG. 1. Three-dimensional plot of logarithmic absolute numbers of electrons emitted at 0° from carbon foils after H^0 and H^+ (3 MeV) impact, as a function of the target thickness ρx [11].

 ©1991 The American Physical Society

the solid by collisions. Part of these electrons emerge from the surface with a velocity distribution centered in the zero-velocity peak, constituting a background spectrum. The ions in the beam capture electrons from this distribution to produce the convoy peak. They find that the ratio between this "intrinsic" convoy-electron (ICE) peak height to the background yield (BE), for $\mathbf{v}=\mathbf{v}_i$, is almost independent of the target thickness, as shown in Fig. 2(b). Barrachina *et al.* [13] assume that convoy electrons are produced inside the target by the ELC process and suffer elastic and inelastic collisions with the atoms before exit. This gives a general description of the forward spectrum but does not give a constant ratio between convoy and background electrons as obtained by Yamazaki and Oda [12].

In this paper we introduce a transport theory for the problem. We consider that the ion–solid-foil interaction can be modeled as a beam which collides with a gas medium. The transport equation that we study is obtained starting from the Boltzmann equation for several species with creation and removal events [14].

We analyze the allowed channels in the beam-gas collision and introduce some simplifying assumptions. The electrons are supposed to be produced by ELC and ECC inside the medium, and are scattered and lose energy by elastic and excitation collisions with the atoms of the medium.

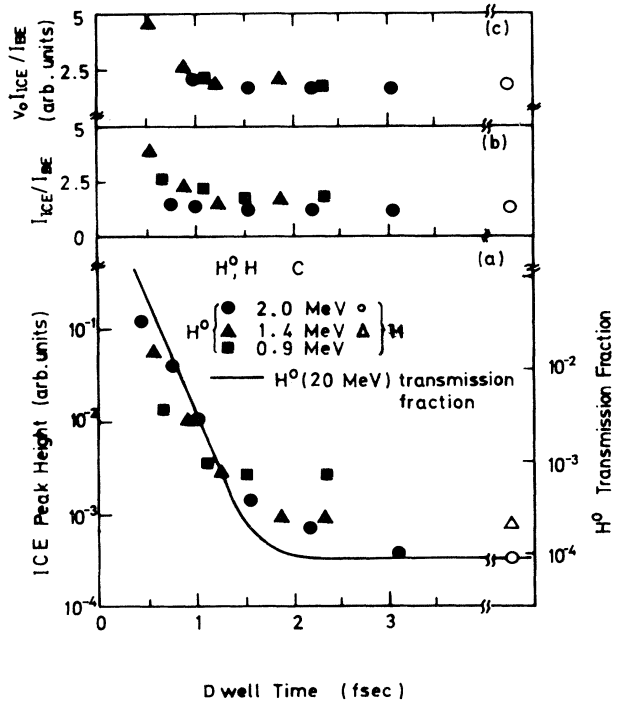

FIG. 2. (a) The ICE peak height; (b) the ratio of ICE peak height to the BE intensity at the ICE peak energy, $I_{\mathrm{ICE}}/I_{\mathrm{BE}}$; and (c) the modified ratio $v_i I_{\mathrm{ICE}}/I_{\mathrm{BE}}$ as functions of dwell time [12].

II. TRANSPORT EQUATION FOR THE DISTRIBUTION FUNCTION

We consider a mixed beam of atoms and ions which collides with a medium of atoms at rest. We will consider the stationary regime. The Boltzmann equation describing the evolution of the distribution function of each species i, without external forces, is

$$\mathbf{v}\cdot\nabla f_i=\sum_{j=1}^{N} B[f_i,f_j] \tag{1}$$

with

$$B[f_i,f_j]=\int d\mathbf{w}\,d\mathbf{v}'d\mathbf{w}'W^{ij}(\mathbf{v},\mathbf{w}|\mathbf{v}',\mathbf{w}') \times[f_i(\mathbf{v}',\mathbf{x},t)f_j(\mathbf{w}',\mathbf{x},t) -f_i(\mathbf{v},\mathbf{x},t)f_j(\mathbf{w},\mathbf{x},t)]+S \tag{2}$$

where S represents sources, N is the number of species, $W^{ij}(\mathbf{v},\mathbf{w}|\mathbf{v}',\mathbf{w}')$ is the transition probability for the ij reaction channel, which can be expressed in terms of the corresponding differential cross section $d\sigma^{ij}(g,\mathbf{g}\cdot\mathbf{g}')/d\mathbf{v}$, $\mathbf{v}$ and $\mathbf{w}$ are the velocities before collision, and $\mathbf{v}'$ and $\mathbf{w}'$ those after collision. The $\mathbf{v}$, $\mathbf{w}$, $\mathbf{v}'$, and $\mathbf{w}'$ are connected by the laws of conservation of momentum and energy. We call $\mathbf{g}=m_i\mathbf{v}-m_j\mathbf{w}$ and $\mathbf{g}'=m_i\mathbf{v}'-m_j\mathbf{w}'$ the relative momentum of particles, where m_i and m_j are the masses of particles.

The bulk plasmon peak has not been observed in the lower-energy side of the cusp-shaped spectra [15]. Then, as in Refs. [11] and [13], we will not consider the collective oscillations or plasmons of the dense electron gas of a solid in the volume. The model here proposed only includes collision between individual particles.

The involved species are ions (I) and atoms that travel with the beam (A), atoms at rest (B) and electrons (e).

The possible collisions channels are as follows:

(a) $I+B\rightarrow I+B$ elastic diffusion (σ^{ei}),
(b) $I+B\rightarrow I+B^{+}+e$ ionization (σ^{i}),
(c) $I+B\rightarrow A+B^{+}$ electron capture (σ^{r}),
(d) $I+B\rightarrow I+B^{*}$ excitation (σ^{*}_{if}), [
(e) $A+B\rightarrow A+B$ elastic diffusion (σ^{ea}),
(f) $A+B\rightarrow A+B^{+}+e$ ionization (σ^{ia}),
(g) $A+B\rightarrow A+B^{*}$ excitation (σ^{*a}_{if}),
(h) $A+B\rightarrow I+B+e$ electron loss (σ^{el}),
(i) $e+B\rightarrow e+B$ elastic diffusion (σ^{ee}),
(j) $e+B\rightarrow e+B^{*}$ excitation (σ^{*e}_{if}), and
(k) $e+B\rightarrow e+B^{+}+e$ ionization (σ^{ie}), where we indicate in parentheses the notation we will use for the respective cross sections.

We assume that the convoy electrons are produced inside the solid, when the ions and atoms in the beam collide with nonexcited target atoms at rest, by electron loss and capture to continuum processes. These convoy electrons act as a beam of electrons inside the solid and modify their velocity in magnitude and direction by inelastic and elastic collisions with target atoms. These collisions inside the solid are represented by the channels (i)–(k).

The electron distribution has axial symmetry around the incident beam direction, along the x axis normal to the foil. The beam is wide and the variation of the elec-

tron distribution will only be in the x direction. Therefore the evolution equation for the distribution function of the electrons is

$$v_x \frac{\partial f_e}{\partial x} = H(\mathbf{v},x) - P(\mathbf{v}) f_e(\mathbf{v},x) + G(\mathbf{v},x) \ . \tag{3}$$

The function $H(\mathbf{v},x)$ represents the electron source:

$$H(\mathbf{v},x) = n_I n_B \frac{d\sigma^i}{d\mathbf{v}} + n_A n_B \frac{d\sigma^{el}}{d\mathbf{v}} \ . \tag{4}$$

$\mathbf{v}_i$ is the beam velocity, n_A and n_I are the charge fractions of the neutral atoms and ions in the beam, respectively; n_B is the density of atoms at rest in the target. The differential cross sections, $d\sigma^i/d\mathbf{v}$ and $d\sigma^{el}/d\mathbf{v}$, correspond to channels (b) and (h), described above, respectively.

We define the spatial variable $x' = n_B x$ and from now on we note $x' \to x$.

The functional form of n_A has been obtained by Allison [16]:

$$n_A(x) = n_A(\infty)(1 - e^{-(\sigma^{el}+\sigma^r)x}) + n_A(0) e^{-(\sigma^{el}+\sigma^r)x} \tag{5}$$

where

$$\begin{aligned} n_A(\infty) &= [\sigma^r/(\sigma^r+\sigma^{el})] n_H \ , \\ n_I(x) &= n_H - n_A(x) \ . \end{aligned} \tag{6}$$

If we analyze the collision between the electron and the target atoms, the conservation equations of momentum and energy are

$$\mathbf{v}' + M\mathbf{w}' = \mathbf{v} + M\mathbf{w} \ , \tag{7}$$

$$v'^2 + Mw'^2 + 2E_i = v^2 + Mw^2 + 2E_f \ . \tag{8}$$

M is the target mass and E_i and E_f are the electronic energies in the initial state and the excited final state f, respectively. We use atomic units.

The function $P(\mathbf{v})$ accounts for the loss of electrons of velocity $\mathbf{v}$ by elastic and inelastic collisions between electrons and target atoms at rest. It is

$$P(\mathbf{v}) = n_B \int [W^{ee}(\mathbf{v},\mathbf{w}|\mathbf{v}',\mathbf{w}) + \sum_f W^{if}(\mathbf{v},\mathbf{w}|\mathbf{v}',\mathbf{w}')] \times \delta(\mathbf{w}) d\mathbf{w}\, d\mathbf{v}'\, d\mathbf{w}' \tag{9}$$

with

$$W^{ee}(\mathbf{v},\mathbf{w}|\mathbf{v}',\mathbf{w}') = g \frac{d\sigma^{ee}(g,\mathbf{g}\cdot\mathbf{g}')}{d\mathbf{v}'} \delta(\mathbf{v}' + M\mathbf{w}' - (\mathbf{v} + M\mathbf{w})) \times \delta(v'^2 + Mw'^2 - (v^2 + Mw^2)) \tag{10}$$

and

$$W^{if}(\mathbf{v},\mathbf{w}|\mathbf{v}',\mathbf{w}') = g \frac{d\sigma^{*e}_{if}(g,\mathbf{g}\cdot\mathbf{g}')}{d\mathbf{v}'} \delta(\mathbf{v}' + M\mathbf{w}' - (\mathbf{v} + M\mathbf{w})) \times \delta(v'^2 + Mw'^2 - (v^2 + Mw^2 + \Delta E_{if})) \ . \tag{11}$$

ΔE_{if} is the energy difference between the final f and initial i states, $d\sigma^{ee}/d\mathbf{v}'$ is the elastic differential cross section, and $d\sigma^{*e}_{if}/d\mathbf{v}$ is that for inelastic processes including excitation and ionization of target atoms by electronic impact.

The loss term, considering elastic and inelastic processes, may be calculated from (9)–(11), resulting in

$$P(\mathbf{v}) = v \left[\sigma^{ee}(v) + \sum_f \sigma^{*e}_{if}(v) \right] \tag{12}$$

in terms of the total cross sections.

The function $G(\mathbf{v},x)$ considers the gain of electrons of velocity $\mathbf{v}$, produced by the above-mentioned processes, and is

$$G(\mathbf{v},x) = G^e + G^i = G^e + \sum_f G^{if} \ . \tag{13}$$

G^{if} are the inelastic gains:

$$G^{if} = n_B \int f_e(\mathbf{v}',x) \delta(\mathbf{w}') W^{if}(\mathbf{v},\mathbf{w}|\mathbf{v}',\mathbf{w}') d\mathbf{w}\, d\mathbf{v}'\, d\mathbf{w}' \ . \tag{14}$$

G^e is the elastic one:

$$G^e = n_B \int f_e(\mathbf{v}',x) \delta(\mathbf{w}') W^e(\mathbf{v},\mathbf{w}|\mathbf{v}',\mathbf{w}') d\mathbf{w}\, d\mathbf{v}' d\mathbf{w}' \ . \tag{15}$$

Equations (3), (4), (9), and (13) determine the spatial evolution of the distribution function. These equations are similar to those in the beam slow down; the main difference is the source term.

In the following we discuss the simplest model which can describe the experimental data considering the excitation channels alone. At present, a better quantitative and realistic description including the electron-atom ionization channel appears to be a formidable task, even though highly desirable, in view of the mathematical complexity that it introduces. Corrections due to the ionization processes are therefore an open question and presently under investigation. We focus here on the influence of the atom-excitation channels on the transport of the electrons.

We consider that the excitation cross section mainly contributes for small dispersion angles [17] and we do not take into account the atomic recoil. The final form of $G^i(\mathbf{v},x)$ is

$$G^i(\mathbf{v},x) = \sum_f f_e((v^2 + 2\Delta E_{fi})^{1/2}, \vartheta, x) \times (v^2 + 2\Delta E_{fi})^{1/2} \sigma^{*e}_{if}((v^2 + 2\Delta E_{fi})^{1/2}) \ . \tag{16}$$

σ^{*e}_{if} is the total excitation cross section from the initial state i to a final state f.

The electron velocities considered experimentally are within $7 \le v_i \le 11$ a.u. Meanwhile the excitation energy steps for the outer electrons of C atoms are $\Delta E_{fi} \le 0.4$ a.u. In that case we can approximate $(v^2 + 2\Delta E_{fi})^{1/2} \cong v + \Delta E_{fi}/v$.

If we consider the conservation of momentum and energy equation, the elastic gain term is

$$G^e(\mathbf{v},x) = v \int f_e(v,\Omega',x) \frac{d\sigma^{ee}(v,\Omega,\Omega')}{d\Omega'} d\Omega' \ . \tag{17}$$

Ω' and Ω are the directions of electron motion before and after the collision, respectively.

Assuming that the atoms are initially at the ground state, $i=0$, the approximate equation for the evolution of the electronic distribution function reads

$$v_x\frac{\partial f_e}{\partial x}=H(\mathbf{v},x)-f_e(\mathbf{v},x)v\left[\sum_f\sigma_{0f}^{*e}(v)+\sigma^{ee}(v)\right]+\sum_f f_e((v^2+2\Delta E_{f0})^{1/2},\vartheta,x)\times\sigma_{0f}^{*e}((v^2+2\Delta E_{f0})^{1/2})(v^2+2\Delta E_{f0})^{1/2}+v\int f_e(v,\Omega',x)\frac{d\sigma^{ee}(v,\Omega,\Omega')}{d\Omega'}d\Omega' . \quad (18)$$

This is an evolution equation for the transport inside the solid of the electrons produced by the beam. It provides a simple solvable model, which, however, does not include all the possible processes inside the solid. In the next section we will show that it is able to describe the experimental observations.

III. RESULTS

To solve (18) we have to introduce some assumptions. In the source term $H(\mathbf{v},x)$, we propose that the ionization ($d\sigma^i/d\mathbf{v}$) and the electron loss ($d\sigma^{el}/d\mathbf{v}$) differential cross sections are mainly determined by the Coulomb factor f_c and the soft electron peak. We will assume approximate shapes:

$$\frac{d\sigma^i}{d\mathbf{v}}=s_c f_c v^{-1} , \quad (19)$$

$$\frac{d\sigma^{el}}{d\mathbf{v}}=s_l f_c v^{-1} \quad (20)$$

where

$$f_c=\frac{2\pi Z_p}{|\mathbf{v}-\mathbf{v}_i|}\left[1-\exp\left[-\frac{2\pi Z_p}{|\mathbf{v}-\mathbf{v}_i|}\right]\right]^{-1} , \quad (21)$$

s_c and s_l are constants which are determined by the projectile charge Z_p and target material, and v_i is the beam velocity.

Replacing (5), (6), (19), (20), and (21) in (4), we obtain

$$H(\mathbf{v},x)=f_c h(v,x)/(vv_x) ,$$
$$h(x)=(\gamma e^{-\sigma x}+\beta) , \quad (22)$$

where

$$\beta=(s_c\sigma^{el}+s_l\sigma^r)/\sigma , \quad (23)$$

$$\sigma=\sigma^r+\sigma^{el} . \quad (24)$$

For a neutral initial beam, we have

$$\gamma=(s_l-s_c)\sigma^{el}/\sigma . \quad (25)$$

If there are only ions in the incident beam:

$$\gamma=(-s_l+s_c)\sigma^r/\sigma . \quad (26)$$

Now, we solve (18) using the finite difference method. We study the electron emission in the forward direction, i.e., $\vartheta=0$. In that case the elastic gain can be neglected since there is a small probability that the elastic collision of the electronic beam with the background atoms add particles to that beam.

With that method the electron distribution function reads

$$F_e(v,x_j)=\left[\frac{(\gamma e^{-(\sigma/v_i)x}+\beta)2\pi}{|v-v_i|[1-\exp(2\pi/|v-v_i|)]}-P(v)F_e(v,x_{j-1})+\sum_h F_e(v+\Delta E_{fi}^h/v,x_{j-1})\tau\sigma_h^{*e}(v+\Delta E_{fi}^h/v)(v+\Delta E_{fi}^h/v)\right]\frac{\Delta x}{v}+F_e(v,x_{j-1}) \quad (27)$$

where τ is the parameter that accounts for the truncation of the sum over the excited states, as will be explained below.

The numerical calculation of this equation must omit a neighborhood of the divergent point $v=v_i$. Inside the range $v_i-\delta<v_i<v_i+\delta$ (δ defines a small velocity range), the distribution function is described by an E_c function defined by

$$v_x\frac{\partial E_c}{\partial x}=f_c(\gamma e^{-\sigma x}+\beta)/v-E_c(v,x)P(v) . \quad (28)$$

This E_c approaches the electron distribution for $v\in[v_i-\delta,v_i+\delta]$ and gives the convoy-electron distribution. The solution of (28) is

$$E_c(v,x)=f_c(T+Be^{-[P(v)/v_x]x}+Ce^{-\sigma x})/v , \quad (29)$$

$$T=\frac{\beta}{P(v)} ,$$
$$C=\frac{\gamma}{[P(v)-\sigma v_x]} , \quad (30)$$
$$B=-(T+C) ,$$

where we choose $x=0$ as the entrance surface of the ion beam.

Both solutions must be coupled, that is,

$$f_e(v,x)=\begin{cases}\alpha(\delta)F_e(v,x) , & v<v_i-\delta,\ v>v_i+\delta\\ E_c(v,x) , & v_i-\delta<v<v_i+\delta .\end{cases} \quad (31)$$

To determine the factor $\alpha(\delta)$ we study the electronic density evolution. We start from (18), neglecting elastic gain and making the integration in velocity:

$$\int v\frac{\partial f_e}{\partial x}dv=\int dv\left[H(v,x)-f_e(\mathbf{v},x)P(v)+\sum_f f_e(v+(\Delta E_{fi}/v),x)\times\sigma_f^{*e}(v+(\Delta E_{fi}/v))\times[v+(\Delta E_{fi}/v)]\right].$$

Substituting here the solution (31) it is possible to obtain the equation for $\alpha(\delta)$:

$$\alpha(\delta)=1+\frac{\int_\Delta dv\,G(v,x)dv}{\int' H(v,x)dv}$$

with $\int'=\int_0^{v-\delta}+\int_{v+\delta}^{\infty}$, and $\int_\Delta=\int_{v-\delta}^{v+\delta}$ and $G(v,x)$ is the gain term where f_e is replaced by $E_c(v,x)$. Evaluation shows that $\alpha\cong 1$ to order 10^{-3}, for $\delta\cong 10^{-4}$.

We will compare our model with the experimental data for electron production by a beam of H^0 and H^+ at 3 MeV colliding with carbon foils.

A numerical study of (18) requires the elastic and inelastic cross sections. The differential elastic cross sections is [18]

$$\frac{d\sigma^{ee}}{d\Omega}\propto Z_p^2\Big/\left\{v^4\left[\sin^2\left(\frac{\vartheta}{2}\right)+\nu^2\right]^2\right\}. \tag{32}$$

The screening ν is determined by the Thomas-Fermi model, $d\Omega$ is the differential of solid angle, and Z_p the projectile charge. The total elastic cross section, calculated using the Thomas-Fermi method, is [18]

$$\sigma^{ee}\propto Z^{4/3}/v^2\ . \tag{33}$$

The total excitation cross section for high-energy electron collision in the Bethe [19] description is

$$\sigma_{0f}^{*e}=(a_f\ln E+b_f)/E\ . \tag{34}$$

a_f and b_f are related to the oscillator strength, and for optically forbidden transitions $a_f=0$.

Lacking experimental data for the excitations of C atoms by electron impact, we consider the theoretical results obtained by Ganas [20] for the transitions $2p$-ns, $2p$-nd, and the optically, forbidden $2p$-np, when collision electron incident energies are smaller than 5 KeV. We do a Fano plot from the curves describe by Ganas and by a least-squares fit we obtain, for each transition, the a_f and b_f values. These values are

$2p$-	a_f	b_f	ΔE_{fi} (a.u.)
$4s$	0.127	0.219	0.3559
$5s$	0.0363	0.0915	0.3822
$3p$	0.0	3.2	0.3370
$4p$	0.0	0.852	0.3705
$3d$	1.114	0.234	0.3614
$4d$	0.525	0.0225	0.3832
$5d$	0.235	0.164	0.3941

However, the remaining excitation transitions cannot be neglected. We assume that they can be taken into account by a factor τ that multiplies the theoretical value of σ_{0f}^{*e}, in first approximation. Therefore the inelastic mean free path is given by

$$\lambda_i\cong 1/\left[\tau\sum_f\sigma_{0f}^{*e}(v_i)\right].$$

For free electrons in C $\lambda_i\cong 17$ Å (for $v_i=10.96$ a.u.) and it results in $\tau\cong 2.25$, but this value is not applicable to the convoy electrons considered here, and τ should be assumed as an additional parameter. This maintains the energy dependence given by (34). The transport length for the convoy electrons is

$$\lambda_c=v_x/P(v)=(\lambda_e^{-1}+\lambda_i^{-1})^{-1}\ .$$

In the source term we adopt for σ^r, σ^{el}, α_c, and α_l the values given by Koschar *et al.* [11], that is

$$\sigma_c=3\times10^{-21}\ \text{cm}^2/\text{at.}\ ,\quad \sigma_l=14.1\times10^{-18}\ \text{cm}^2/\text{at.}\ ,$$

$$\alpha_c=0.024\ ,\quad \alpha_l=0.097\ ,$$

which we relate to s_c and s_l by

$$s_c=L\alpha_c\sigma^r\ ,\quad s_l=L\alpha_l\sigma^{el}\ .$$

For comparison with the experiment the distribution must be convoluted with the resolution of the equipment. We make this convolution using the method of Dettman, Harrison, and Lucas [2] considering the angular resolution of 0.1° and a momentum resolution of 0.7%. We denote by $F(v,x)$ and $E(v,x)$ the distributions resulting from the convolution of $F_e(v,x)$ and $e_c(v,x)$, respectively.

Comparison of $E(v,x)$ with the experimental convoy-electron yield at $x\to\infty$ gives $L=6$ and $\lambda_c=6.2$ Å. In Fig. 3 we graph the function E with the above coefficients; it fits the absolute number of the intrinsic convoy-electron (ICE) yield; the experimental points correspond to Ref. [11].

A value for the e-C elastic cross section must be fixed in (17). No experimental determination is available and we use the value given by a first-order perturbative approximation in the Thomas-Fermi model. This gives $\sigma^{ee}=0.37$ a.u., that is, $\lambda_e=100$ Å, at the considered energy.

In Fig. 4 we show the calculated electron distribution function for the collision of H^0, at 3 MeV, with carbon foils of different thicknesses. Figure 5 shows the good agreement of the resulting electron distribution with the experimental values. When the foil is sufficiently thin, only the known convoy-electron peak is observed; meanwhile, when the target thickness increases, a second structure begins to appear, which shifts to the region of lower velocities. This structure is caused by the convoy electrons produced inside the solid, by electron loss or capture processes, which lose their initial energy by inelastic collision. Furthermore they are elastically scattered by the target atoms. When the foil thickness is sufficiently large the number of collisions is so high that the scattered electrons may be thermalized. Then they only contribute to the low-energy electron spectrum. In

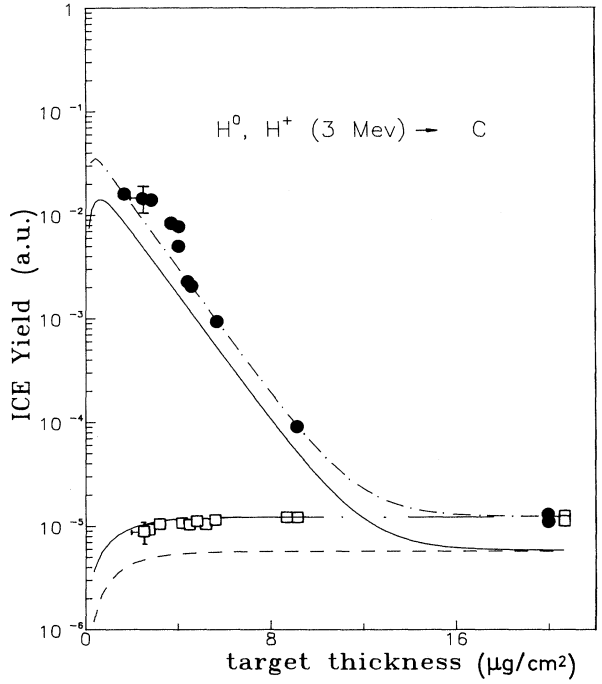

FIG. 3. ICE yield per incident projectile of H^0 (solid circle [11]): — —, present model; ——, Ref. [11]; and H^+ (open square): — —, present model; – –, Ref. [11].

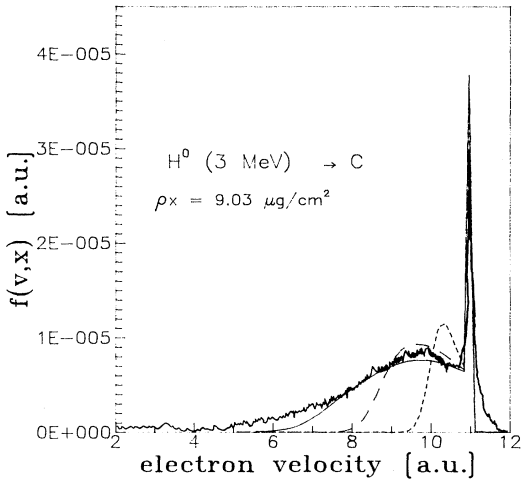

FIG. 5. Comparison of the convoluted electron distribution of H^0 (3 MeV) traversing a carbon foil of $\rho x = 9.03$ μg/cm described by the present model with the experimental curve of Ref. [11]: ——, with $\lambda_c = 6.2$ Å, $L = 6$; – – –, with $\lambda_c = 8.6$ Å, ---, $L = 4$; and with $\lambda_c = 16.4$ Å, $L = 1.9$.

that case again only the convoy structure appears, but with a much smaller intensity.

It is very interesting to note the good qualitative accord between the form of the nonconvoy-electron (NCE) spectrum, described by Yamazaki [15], and our calculations. The NCE's, also called background electrons (BE), are characterized by the function F which is graphed in Fig. 6.

Now we are interested in the analysis of the relation between the intrinsic convoy electrons, characterized by the function E, with "background" electrons, given by F. In Fig. 7 we represent, for different target thicknesses, the ratio $E(v_i - \delta, x)/F(v_i - \delta, x)$. It is observed that this ratio is constant when the thickness is larger than a certain value.

In Fig. 8 we describe the collision of H^+ with C foil of

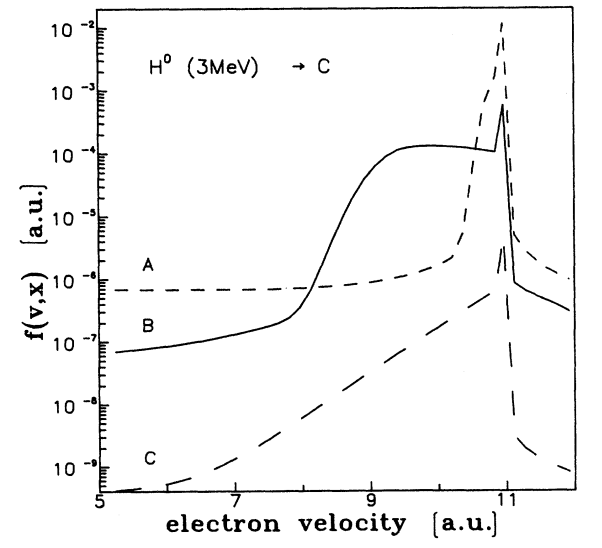

FIG. 4. Logarithmic convoluted electron distribution considering an angular resolution of 0.1° and a momentum resolution of 0.7% of H^0 (3 MeV) traversing carbon foil as function of electron velocity, for different thicknesses. A: $\rho x = 0.71$ μg/cm^2; B: $\rho x = 4.98$ μg/cm^2; C: $\rho x = 26.12$ μg/cm^2.

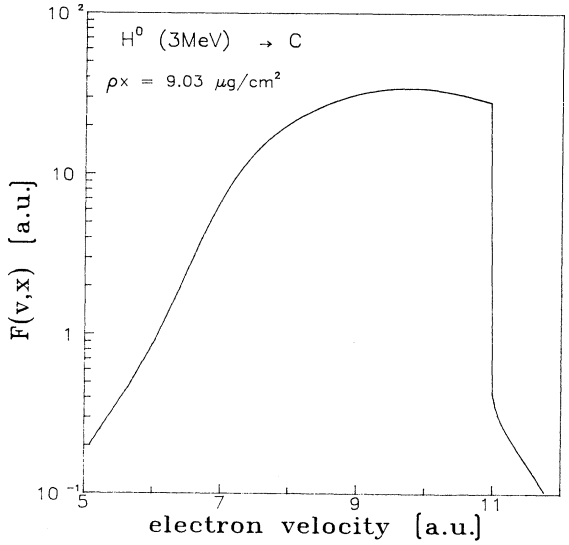

FIG. 6. BE distribution H^0 (3 MeV) traversing a carbon foil of $\rho x = 9.03$ μg/cm^2 as function of electron velocity.

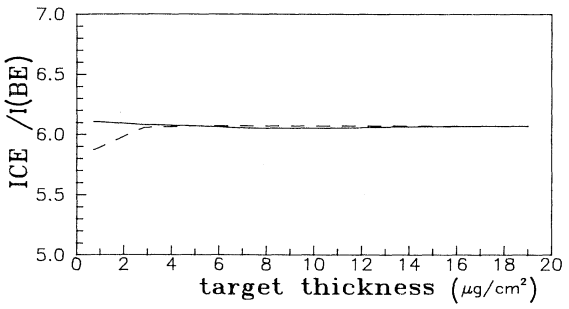

FIG. 7. The ratio of ICE peak height to the BE intensity at the ICE peak velocity, ICE/BE, as function of target thicknesses ($\mu g/cm^2$). ——: $H^+ \rightarrow C$; – – –: $H^0 \rightarrow C$.

different thicknesses. When the target thickness is increased, we observe that the second displaced structure mentioned above appears again. It is also produced by the collision of a convoy electron with the target atoms. Because of the absence of direct electron loss to continuum in $H^+ + C$ collision, the ICE yield for H^+ never decreases, and the displaced structure does not have a maximum. Upon further increase of thickness the peak form does not change anymore. Note that, for a sufficiently thick C foil, the electron spectrum is almost equal for H^0 or H^+ beams (curves *C* in Figs. 4 and 8).

IV. CONCLUSIONS

In this paper it has been possible, using a transport theory, to describe the experimentally observed structure of electron spectra obtained when H^0 and H^+ collide with C foils of different thicknesses.

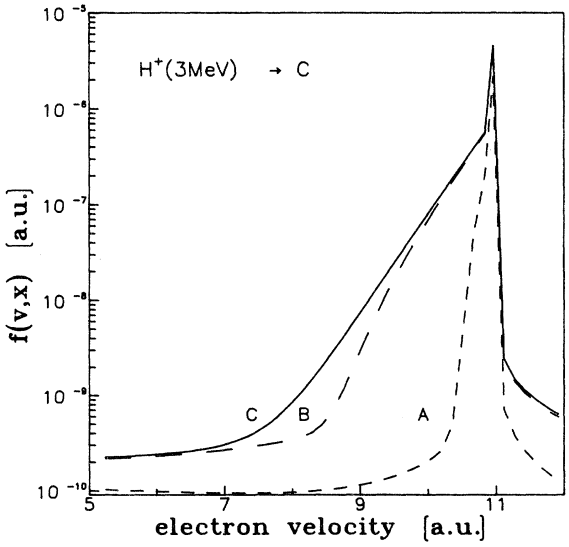

FIG. 8. Logarithmic convoluted electron distribution of H^+ (3 MeV) traversing a carbon foil as function of electron velocity, for *A*: $\rho x = 0.71\ \mu g/cm^2$; *B*: $\rho x = 4.98\ \mu g/cm^2$; *C*: $\rho x > 9.03\ \mu g/cm^2$.

Starting from a generalized Boltzmann equation, and considering that the differential cross sections of electron loss and ionization, are mainly determined by the Coulomb factor, we study the H^0-C foil collision. We describe, in good qualitative accord with the experiment, the electron spectrum for different target thicknesses. Studying the collision of H^+ with carbon foil, we observe that, when the target thicknesses increase, the displaced structure appears again, but it is less pronounced and does not have a maximum. This effect has not been experimentally observed yet. The peak form does not change, if the thickness continues to grow.

Furthermore, with this model for the production of convoy electrons inside the solid, we obtain the same constant behavior of the ratio between the ICE's and BE's which has been observed by Yamazaki and Oda [12]. We think that it is possible to describe this ratio because the electron distribution functions are deduced starting from a generalized transport equation, which considers all the processes in one and the same equation. Therefore it is not necessary to introduce *ad hoc* a Landau function [11–13], which describe the inelastic processes.

In the present model we calculate the parameters in such a way that the ICE yield could describe the experimental data. We realize that the value considered for the elastic mean free path λ_e is greater than that corresponding to free electrons in C foil. In (18) we neglected the elastic gain term at zero degree, which could compensate an actually smaller value of λ_e.

Note also that the comparison with the experiment is better when the value for the inelastic mean free path, λ_i, is smaller than for the free electron. This may be attributed to the interaction of the convoy electron with the projectile, in accordance with the concept of Coulomb defocusing. In particular, in Fig. 7 of Ref. [21], it is observed that the convoy-electron population is depleted rapidly, in a collection volume which covers the longitudinal interval $v_i \pm 0.25$ and a transversal width $v_T = 0.25$, in comparison with the free electron population. This can be attributed to the fact that a single collision is enough in most cases to remove an electron from the collection volume, because of the relatively large energy transfer per collision [21]. The inclusion of the projectile effect requires an additional term in the Boltzmann equation (1) to consider the external force applied to the electron distribution. This study, in a classical theory scheme, as presented here, implies the introduction of a time- and space-dependent potential which must be calculated in a self-consistent form. At this first stage of our analysis, it has not been considered because of the great complexity that it introduces in the transport equation.

The total mean free path λ_c is mainly determined by the λ_i. For incident H^0, λ_c determines the target thicknesses for which the ICE yield reaches the maximum value; this maximum position is independent of the value of L (Fig. 9). It would be interesting to perform an experiment to determine this total mean free path. For this purpose, the maximum of the ICE yield would have to be measured with H^0 on dense gases at velocities $v_i \cong 1$ or 2 a.u. or on C foils with beam velocities $v_i \gg 10$ a.u. Experiments like these have already been proposed but

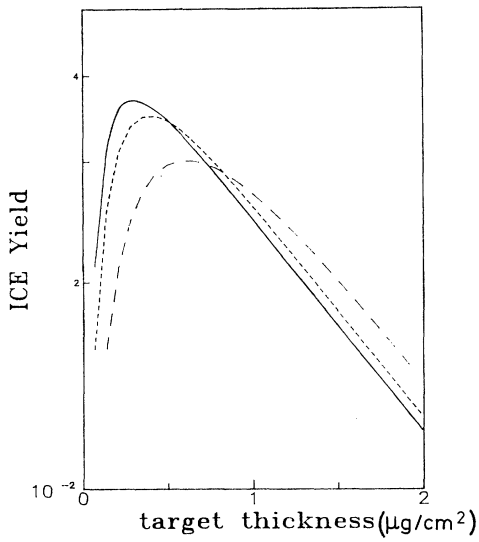

FIG. 9. ICE yield per incident projectile of H^0 (3 MeV) on C foil as a function of target thicknesses ($\mu g/cm^2$), for different values of the total mean free path. ——: $\lambda_c = 6.2$ Å, $L = 6$; --- $\lambda_c = 8.6$ Å, $L = 4$; – – – $\lambda_c = 16.4$ Å, $L = 1.9$.

not performed yet, probably due to the experimental difficulties. Therefore we believe useful a reexamination of the intermediate thicknesses in order to obtain the inflection point of the ICE yield. Like the maximum point, the inflection point is also directly related to λ_c. A determination of λ_c in this way would shed some light on the effect of the projectile when the transport of convoy electrons in the solid is studied.

In the present model we have not included some surface effects. This is because, in the velocity range considered here, no modifications in the convoy-electron spectra, as due to the exit surface potential [22,23], are observed experimentally.

All the results described above could be improved if we consider the contribution from ionization of the atoms at rest, by electron impact. Furthermore, the interactions of beam electrons with the electrons of the plasma would be included. In the present deductions of the transport equation, this would introduce a nonlinear behavior. Nevertheless, a completely different method exists to evaluate the energy loss of electrons interacting with solids. It is connected with the dielectric properties of the material, and it has been successfully employed in calculations of energy loss distribution for electrons transmitted through a thin layer of carbon [24–26]. The dielectric description of slowing down may be considered as an alternative to the Bethe deduction of cross section [27], which allows an analysis of the effects of collective excitations.

ACKNOWLEDGMENTS

We would like to thank Dr. W. Meckbach, Dr. R. Barrachina, and Dr. D. Zanette for critical reading of the manuscript and for helpful comments.

[1] W. Meckbach and P. Focke, Nucl. Instrum. Methods B **33**, 255 (1988).
[2] K. Dettmann, K. G. Harrison, and M. W. Lucas, J. Phys. B **7**, 269 (1974).
[3] V. H. Ponce and W. Meckbach, Comments At. Mol. Phys. **10**, 231 (1981).
[4] V. N. Neelavathi, R. Ritchie, and W. Brandt, Phys. Rev. Lett. **33**, 302 (1974).
[5] Y. Yamazaki and N. Oda, Nucl. Instrum. Methods **194**, 415 (1982).
[6] R. Latz, G. Aster, H. J. Frischkorn, P. Koschar, J. Pfenning, J. Schader, and K. O. Groeneveld, Nucl. Instrum. Methods **194**, 315 (1982).
[7] R. Latz, J. Schader, H. J. Frischkorn, K. O. Groeneveld, D. Hofmann, and P. Koschar, Z. Phys. A **304**, 367 (1982).
[8] R. Latz, J. Schader, H. J. Frischkorn, P. Koschar, D. Hofmann, K. O. Groeneveld, and W. Meckbach, Nucl. Instrum. Methods B **2**, 265 (1984).
[9] H. P. Hülskötter, J. Burgdörfer, and I. A. Sellin, Nucl. Instrum. Methods B **24/25**, 147 (1987).
[10] P. Koschar, G. Szabó, A. Clouvas, J. Kemmler, O. Heil, C. Biedermann, H. Rothard, K. Kroneberger, S. Lencinas, and K. O. Groeneveld, J. Phys. (Paris) Colloq. **48**, C9-275 (1987).
[11] P. Koschar, A. Clouvas, O. Heil, M. Burkhard, J. Kemmler, and K. O. Groeneveld, Nucl. Instrum. Methods B **24/25**, 153 (1987).
[12] Y. Yamazaki and N. Oda, Phys. Rev. Lett. **52**, 29 (1984).
[13] R. O. Barrachina, A. Goñi, P. Focke, and W. Meckbach, Nucl. Instrum. Methods B **33**, 330 (1988).
[14] M. L. Martiarena and C. R. Garibotti, Physica A **166**, 115 (1990); C. Spiga, T. Nonnenmacher, and V. C. Boffi, *ibid.* **131**, 431 (1985).
[15] Y. Yamazaki, in *High-Energy Ion-Atom Collision,* edited by D. Berenyi and G. Hock, Lecture Notes in Physics Vol. 294 (Springer-Verlag, Berlin, 1988), p. 321.
[16] S. K. Allison, Rev. Mod. Phys. **30**, 1137 (1958).
[17] N. P. Kalashnikov, V. S. Remizovich, and M. I. Ryazanov, *Collisions of Fast Charged Particles in Solids* (Gordon and Breach, Amsterdam, 1985).
[18] M. F. Mott and H. S. Massey, *The Theory of Atomic Collisions* (Oxford University Press, New York, 1965).
[19] M. Inokuti, Rev. Mod. Phys. **43**, 297 (1971).
[20] P. Ganas, Physica **104C**, 411 (1981).
[21] J. Burgdörfer, in *High-Energy Ion-Atom Collision* (Ref. [15]), p. 344.
[22] E. Sanchez, Nucl. Instrum. Methods A **280**, 433 (1989).
[23] E. Sanchez *et al.*, Nucl. Instrum. Methods B **43**, 29 (1989).
[24] J. C. Ashley, J. J. Cowan, R. H. Ritchie, V. E. Anderson, and J. Hoelzl, Thin Solid Films **60**, 361 (1971).

[25] J. Kemmler, S. Lencinas, P. Koschar, O. Hiel, H. Rothard, K. Kroneberg, Gy. Szabo, and K. O. Groeneveld, Nucl. Instrum. Methods B **33**, 317 (1988).
[26] S. Lencinas, J. Burgdörfer, J. Kemmler, O. Hiel, K. Kroneberger, H. Rothard, and K. O. Groeneveld, Phys. Rev. A **41**, 1435 (1990).
[27] E. Bonderup, *Penetration of Charged Particles Through Matter* (University of Aarhus, Aarhus, Denmark, 1974).